
Journal of the
HYDRAULICS DIVISION
Proceedings of the American Society of Civil Engineers

TRANSIENT HYDRAULIC SIMULATION OF BREACHED EARTH DAMS

By Danny L. Fread¹ and Terence E. Harbaugh,² Members, ASCE

INTRODUCTION

Numerous small homogeneous earthfill dams, up to approximately 100 ft in height, have failed or are subject to possible failure from overtopping because of inadequate spillways (12,17). Such failures may cause considerable property damage and even the loss of life. Middlebrooks (12) states that prior to 1950 approximately 220 earth dams in the United States had failed; 30 % of the failures were attributed to overtopping. In Missouri, during the last 10 yr, there have been 17 failures of earth dams and, of these, 10 were due to inadequate spillways, or over-topping; or both. Also, the Missouri Geological Survey (17) considers 39 dams to be potential failures of which 24 are so classified because of inadequate spillways. The inadequate spillways prevalent on many dams generally are due to the lack of engineering consultation during design and construction. As some states are lacking a code for the design of small dams, this paper is directed toward the problem of improving the safety of future dams in those states without requiring the builders to incur engineering costs or the alternate expense of providing over-sized spillway structures.

A conceptual method of alleviating downstream damages from small breached earthfill dams which receive little or no engineering design is to provide a relatively thin erosion retarding layer at an optimal elevation during the construction of the dam. Thus, in the event of an overtopping of the dam, the resulting breach would not develop continuously but would be delayed by the proposed erosion retarding layer. Such a controlled breach would produce two flood waves, each having a reduced amplitude compared to the single flood wave produced by a breach of an earth dam without a retarding layer. Con-

Note.—Discussion open until June 1, 1973. To extend the closing date one month, a written request must be filed with the Editor of Technical Publications, ASCE. This paper is part of the copyrighted Journal of the Hydraulics Division, Proceedings of the American Society of Civil Engineers, Vol. 99, No. HY1, January, 1973. Manuscript was submitted for review for possible publication on May 25, 1972.

¹Hydro., Office of Hydrology-National Weather Service, National Oceanic and Atmospheric Admin., Silver Spring, Md.

²Assoc. Prof. of Civ. Engrg., Dept. of Civ. Engrg., Univ. of Missouri-Rolla, Rolla, Mo.

sequently, some measure of reduction in downstream damages would be obtained.

The hydraulic characteristic of transient reservoir flow resulting from gradually breached earthfill dams are investigated herein to ascertain the potential of the erosion retarding layer for reducing the flood produced by a gradually breached earthfill dam. Simplifications of the geometric and dynamic aspects of the phenomenon are made in order to develop a generalized numerical simulation model of the transient reservoir flow produced by a breached dam. A general model is sought so that the flood reduction benefits of an erosion retarding layer can be assessed in an overall manner rather than be restricted to a limited number of particular prototypes. Thus, the numerical model is used to determine the expected reduction in outflow due to a single retarding layer for several pertinent geometric, dynamic, and hydraulic parameters. Also, the elevation of the retarding layer is optimized so that the maximum possible outflow from a gradually breached dam is minimized.

THEORY

St. Venant Differential Equations.—The basis for formulating a numerical simulation model of the unsteady reservoir flow due to a gradually breached dam is the one-dimensional differential equations of gradually varied, unsteady channel flow. These equations are attributed to A.J.C. Barre'de Saint-Venant and are known as the St. Venant equations. Their derivation is reviewed in several references (4,13,15) and is simply stated herein as

$$\frac{\partial y}{\partial t} + D \frac{\partial v}{\partial x} + v \frac{\partial y}{\partial x} = 0 \dots\dots\dots (1)$$

$$\frac{\partial v}{\partial t} + v \frac{\partial v}{\partial x} + g \frac{\partial y}{\partial x} + g(S_f - S_o) = 0 \dots\dots\dots (2)$$

in which y = depth of flow in the channel; v = average velocity across a section of channel; D = hydraulic mean depth which is equivalent to A/T ; T = width of the free water surface; A = cross-sectional area; g = acceleration due to gravity, x = distance along the channel; t = time; and S_o = slope of the reservoir bottom. The friction slope, S_f , is given by Manning's equation for steady uniform flow. Thus

$$S_f = \frac{n^2 |v|v}{2.21 R^{4/3}} \dots\dots\dots (3)$$

in which n = the Manning coefficient and the hydraulic radius $R = A/P$.

The St. Venant equations are derived from the principles of conservation of mass and momentum. Eq. 1 is known as the equation of continuity and conserves the mass of the transient flow. Eq. 2 models the dynamics of the transient flow; it is known as the equation of motion and conserves the momentum of the flow.

Reservoir Geometry.—The reservoir cross section is assumed trapezoidal with side slopes of l : vertical to z : horizontal, as shown in Fig. 1. Only the prismatic portion of the idealized reservoir shown in Fig. 2 is considered to contribute to the outflow released by a breached dam. The storage in the upper reaches of the reservoir provides little contribution to the outflow because accumulated sediment deposits often reduce this storage to a negligible quantity.

Thus, the upstream boundary is located at the upper end of the prismatic reservoir, a distance, L , from the downstream boundary.

The reservoir bottom slope, S_o , is constant and defined as

$$S_o = \frac{\eta}{L'} \dots\dots\dots (4)$$

in which η = the height of the dam and L' = the distance from the downstream boundary to the intersection with the reservoir bottom of a horizontal line drawn

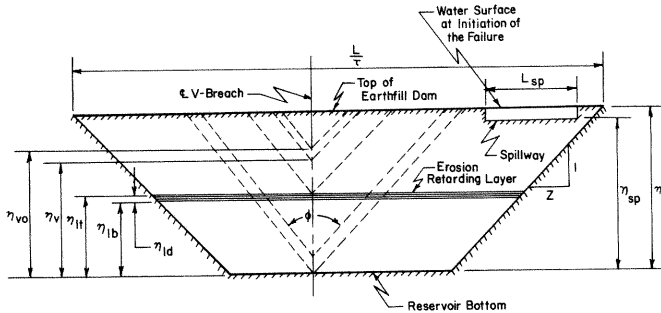


FIG. 1.—RESERVOIR CROSS SECTION WITH EARTHFILL DAM

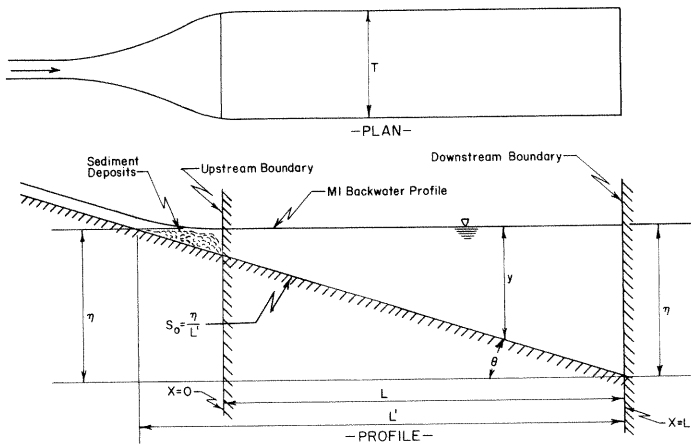


FIG. 2.—IDEALIZED RESERVOIR

from the top of the dam, as shown in Fig. 2. In this investigation, L is defined as

$$L' = K_1 L \dots\dots\dots (5)$$

in which K_1 = a constant.

Breach Geometry and Dynamics.—The breach is assumed to commence forming at the instant the maximum capacity, Q_o , of the emergency or principal

spillway or both, is exceeded and the dam is overtopped. Referring to Fig. 1, the spillway is located at an elevation, η_{sp} , and the breach forms a V where the acute central angle, ϕ , of the V-breach remains constant throughout its formation. This breach geometry is assumed to approximate that caused by the overtopping of a homogeneous earthfill dam (17).

The breach forms at a rate denoted by λ , which is in feet per second, and is defined as the vertical distance traversed by the bottom point of the V-breach during an increment of time. Two basic types of failure rates, λ , are investigated herein. The first type is

$$\lambda = \lambda_c \dots\dots\dots (6)$$

in which λ_c = the constant for a particular interval of time during the failure or for a particular span of vertical distance within the dam; λ may be expressed as a step-function of either time or elevation. For the other type of failure rate, λ = an exponential function of the head of the V-breach, in which the head is defined as $(y_d - \eta_v)$. Thus

$$\lambda = \exp [K_e (y_d - \eta_v)] - 1 \dots\dots\dots (7)$$

in which $K_e = \frac{\ln (1 + \lambda_m)}{y_{dm}} \dots\dots\dots (8)$

and y_d = the transient reservoir depth at the downstream boundary; η_v = the elevation of the bottom of the V-breach; and λ_m and y_{dm} are, respectively, the maximum failure rate and reservoir depth at the downstream boundary when $\eta_v = 0$. When the bottom point of the V-breach is in contact with the erosion retarding layer, the failure rate is significantly reduced to a value of λ/K_λ , where K_λ is a constant greater than unity. The top of the erosion retarding layer is denoted as η_{lt} , the bottom as η_{lb} , and the thickness as η_{ld} .

NUMERICAL SIMULATION MODEL

Dimensional and Geometrical Considerations.—The St. Venant equations are nondimensionalized herein by defining the following dimensionless variables

$$y^* = \frac{y}{\eta}, v = \frac{v}{v_\eta}, x^* = \frac{x}{L}, t^* = \frac{t v_\eta}{L} \dots\dots\dots (9)$$

$$D^* = \frac{D}{D_\eta} = \frac{c_1(c_1 y^* - 2c_2 y^* + c_2 y^{*2})}{(c_1 - c_2)(c_1 - 2c_2 + 2c_2 y^*)} \dots\dots\dots (10)$$

$$R^* = \frac{R}{R_\eta} = \frac{(c_1 - 2c_2 + c_3)(c_1 y^* - 2c_2 y^* + c_2 y^{*2})}{(c_1 - c_2)(c_1 - 2c_2 + c_3 y^*)} \dots\dots\dots (11)$$

in which $c_1 = \frac{L}{\tau}$; $c_2 = z\eta$; and $c_3 = 2\eta \sqrt{1 + z^2} \dots\dots\dots (12)$

and τ = the ratio of the reservoir top width T to the reservoir length, L . The η subscript indicates that the subscripted variable is evaluated at the downstream boundary when $t = 0$, $\eta_v = \eta$. The * superscript is used herein to denote a variable as being dimensionless.

Substitution of Eq. 3 along with the preceding dimensionless variables into

Eqs. 1 and 2, taking care to properly express the partial derivatives, yields the following dimensionless form of the St. Venant equations

$$\frac{\partial y^*}{\partial t^*} + K_1 D^* \frac{\partial v^*}{\partial x^*} + v^* \frac{\partial y^*}{\partial x^*} = 0 \dots\dots\dots (13)$$

$$\frac{\partial v^*}{\partial t^*} + v^* \frac{\partial v^*}{\partial x^*} + K_2 \frac{\partial y^*}{\partial x^*} + \frac{K_3 |v^*| v^*}{R^{*4/3}} - K_4 = 0 \dots\dots\dots (14)$$

in which $K_1 = \frac{(c_1 - c_2)}{c_1} \dots\dots\dots (15)$

$$K_2 = \frac{g\eta^3 (c_1 - c_2)^2}{Q_o^2} \dots\dots\dots (16)$$

$$K_3 = \frac{g\eta^2 L}{2.21^{4/3}} \left[\frac{(c_1 - 2c_2 + c_3)}{(c_1 - c_2)} \right]^{4/3} \dots\dots\dots (17)$$

$$K_4 = \frac{gS_o L\eta^2 (c_1 - c_2)^2}{Q_o^2} \dots\dots\dots (18)$$

Also, the following dimensionless variables are utilized within the model

$$\lambda^* = \frac{\lambda L}{Q_o} (c_1 - c_2), Q_u^* = \frac{Q_u}{Q_o}, Q_d^* = \frac{Q_d}{Q_o} \dots\dots\dots (19)$$

$$\eta_{sp}^* = \frac{\eta_{sp}}{\eta} =, \eta_v^* = \frac{\eta_v}{\eta}, \eta_{lt}^* = \frac{\eta_{lt}}{\eta}, \eta_{lb}^* = \frac{\eta_{lb}}{\eta}, \eta_{ld}^* = \frac{\eta_{ld}}{\eta} \dots\dots (20)$$

The *u* and *d* subscripts refer to the upstream and downstream boundaries, respectively.

The foregoing normalizing procedure allows *y** and η_v^* to take on values from unity to zero and *v** and *Q** to assume values relative to an initial condition of unity. Also, this procedure allows the initial flow, *Q_o*, to be expressed in terms of the dimensionless failure rate, λ^* . This normalizing procedure is utilized for convenience in the presentation of results.

Numerical Solution of St. Venant Equations.—The St. Venant equations defy a closed-form solution; however, they may be solved by numerical techniques such as the explicit method (7,8,14,15), the implicit method (1,3,10,14), and the method of characteristics with a characteristic network (2,9,11,16) and a rectangular network (3,11,14,16). Each of the techniques offer particular advantages and disadvantages. The method of characteristics with a characteristic network is used herein because of its inherent numerical stability, convergence, and the ease with which boundary conditions may be introduced into the solution procedure. Also, the prismatic geometry of the idealized reservoir and the desirability of obtaining solutions at only the upstream and downstream boundaries lend to the selection of the method of characteristics.

Characteristic Equations.—In the method of characteristics (3,11,16), the two St. Venant partial differential equations are converted into four ordinary differential equations, called characteristic equations, which may be numerically integrated subject to specified initial and boundary conditions. Using the method of characteristics, Eqs. 13 and 14 are converted into the following dimensionless characteristic equations

$$\frac{dv^*}{dt^*} - \left(\frac{K_2}{K_1 D^*}\right)^{1/2} \frac{dy^*}{dt^*} + \frac{K_3 |v^*| v^*}{R^{*4/3}} - K_4 = 0, C - \dots \dots \dots (21)$$

$$\frac{dx^*}{dt^*} = v^* - (K_1 K_2 D^*)^{1/2}, C - \dots \dots \dots (22)$$

$$\frac{dv^*}{dt^*} + \left(\frac{K_2}{K_1 D^*}\right)^{1/2} \frac{dy^*}{dt^*} + \frac{K_3 |v^*| v^*}{R^{*4/3}} - K_4 = 0, C + \dots \dots \dots (23)$$

$$\frac{dx^*}{dt^*} = v^* + (K_1 K_2 D^*)^{1/2}, C + \dots \dots \dots (24)$$

Eqs. 21 and 22 are associated with the *C* - characteristic curves in the *x** - *t** solution plane, shown in Fig. 3; Eqs. 23 and 24 are associated with

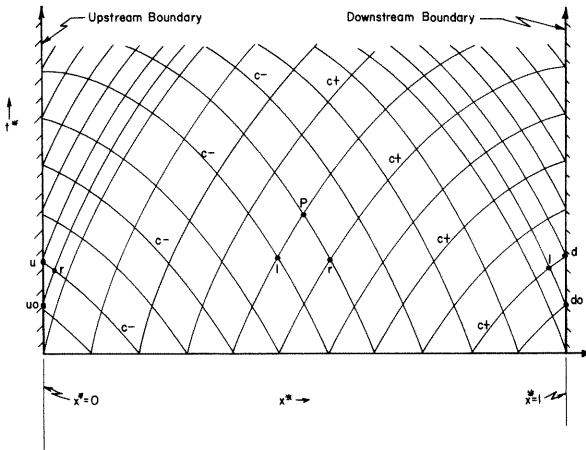


FIG. 3.—*x** - *t** PLANE WITH CHARACTERISTIC NETWORK

the *C* + characteristic curves. Eqs. 21 and 23 are valid only along the curves defined by the *dx*/dt** expressions, Eqs. 22 and 24. All four equations are valid at intersection points, such as *p*, in the *x** - *t** plane. Thus, if the values of *x**, *t**, *y** and *v** are known at points, *l* and *r*, a numerical integration of the equations will produce the values of *x**, *t**, *y**, and *v** at point *p*. In this way, the values associated with all intersection points in the *x** - *t** plane are determined sequentially from left to right while progressing upward in the *t**-direction.

The numerical integration of Eqs. 21-24 may be accomplished by various finite-difference approximations with different orders of accuracy (11). It was found that a first-order approximation provided sufficient accuracy since the variations of *v** and *y** with *x** and *t** are relatively small for a flow produced by a gradual breach. The details of the numerical integration are presented elsewhere (6).

Initial Conditions.—The condition of the flow in the reservoir must be known for solutions to be obtained from the characteristic equations. In this investi-

gation, the initial condition is a steady, gradually varied flow. A step computation (5,6) commencing with the depth in the vicinity of the dam and progressing upstream enables the initial depths and velocities to be computed at finite points along the reservoir.

Upstream Boundary Condition.—The V-breach is assumed to occur during a short duration of time relative to the time base of the reservoir inflow hydrograph. The inflow occurs only at the upper reach of the idealized reservoir such that the reservoir is not subjected to any lateral inflow. Thus, the inflow to the reservoir may be considered relatively constant throughout the formation of the breach, and the upstream boundary condition is expressed in dimensionless form as a constant inflow

$$Q_u^* = \frac{Q_u}{Q_o} = 1 \dots\dots\dots (25)$$

Thus, from continuity considerations

$$v_u^* = \frac{Q_u^* (c_1 - c_2)}{(c_1 y_u^* - 2c_2 y_u^{*2} + c_2 y_u^{*2})} \dots\dots\dots (26)$$

Downstream Boundary Condition.—The downstream boundary condition is given by stage-discharge relationships for the spillway and the V-breach. The elevation of the spillway crest η_{sp}^* is constant, however, the elevation of the bottom of the V-breach η_v^* is a function of t_d , η_{it}^* , η_{ib}^* , and λ^* . The following step-functions express this variation of η_v^* . If $\eta_{vo}^* \geq \eta_{it}^*$, then

$$\eta_v^* = \eta_{vo}^* - \lambda^* (t_d^* - t_{do}^*) \dots\dots\dots (27)$$

however, if $\eta_v^* < \eta_{it}^*$, then $\eta_v^* = \eta_{it}^* - \frac{[\lambda^* t_d^* - (\eta_{vo}^* - \eta_{it}^*)]}{K_\lambda} \dots\dots\dots (28)$

If $\eta_{ib}^* \leq \eta_{vo}^* < \eta_{it}^*$, then $\eta_v^* = \eta_{vo}^* - \frac{\lambda^*}{K_\lambda} (t_d^* - t_{do}^*) \dots\dots\dots (29)$

however, if $\eta_v^* < \eta_{ib}^*$, then $\eta_v^* = \eta_{ib}^* - [\lambda^* t_d^* - K_\lambda (\eta_{vo}^* - \eta_{ib}^*)] \dots\dots (30)$

If $o \leq \eta_{vo}^* < \eta_{ib}^*$, then $\eta_v^* = \eta_{vo}^* - \lambda^* (t_d^* - t_{do}^*) \dots\dots\dots (31)$

however, if $\eta_v^* < o$, then $\eta_v^* = 0 \dots\dots\dots (32)$

The second subscript, *o*, indicates that the subscripted variable is the previously computed boundary point as shown in Fig. 3.

The velocity at the downstream boundary is expressed in terms of the discharges of the spillway and the V-breach and the reservoir cross-section:

$$v_d^* = \frac{[K_5 (y_d^* - \eta_v^*)^{5/2} + K' K_6 (y_d^* - \eta_{sp}^*)^{3/2}] (c_1 - c_2)}{(c_1 y_d^* - 2c_2 y_d^{*2} + c_2 y_d^2)} \dots\dots\dots (33)$$

in which $K' = 1$ if $y_d^* > \eta_{sp}^* \dots\dots\dots (34)$

and $K' = 0$ if $y_d^* < \eta_{sp}^* \dots\dots\dots (35)$

and $K_5 = \frac{C_v \eta^{5/2}}{Q_o} \dots\dots\dots (36)$

$$K_8 = \frac{C_{sp} \eta^{3/2}}{Q_0} \dots \dots \dots (37)$$

$$C_v = 4.28 c_v \tan \frac{\phi}{2} \dots \dots \dots (38)$$

$$C_{sp} = 5.36 c_{sp} L_{sp} = \frac{Q_0}{[\eta(1 - \eta_{sp}^*)]^{3/2}} \dots \dots \dots (39)$$

Term C_v , the coefficient of discharge for the V-shaped breach, incorporates the effects of breach geometry and flow resistance. Term C_{sp} is the discharge

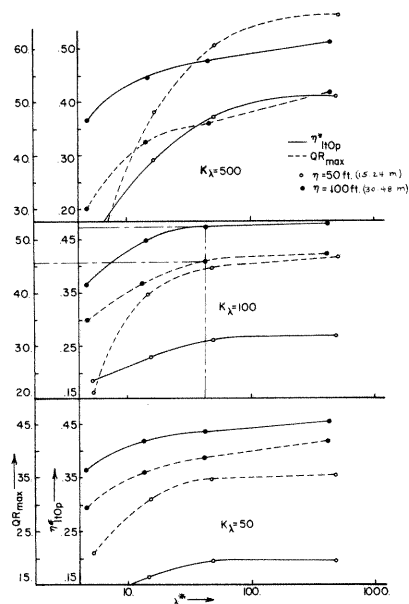
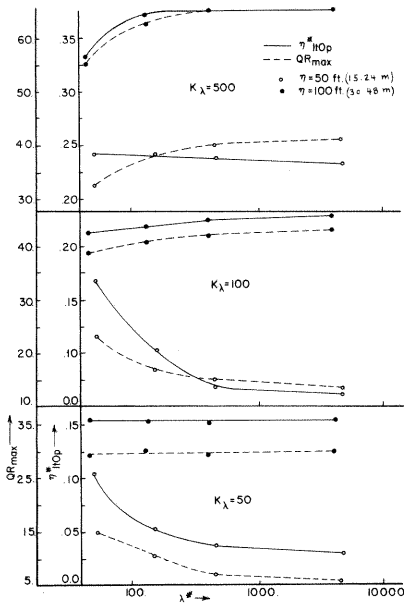


FIG. 4.—RELATIONSHIP BETWEEN QR_{max} AND η_{ltOp}^* FOR VARIOUS VALUES OF λ^* AND $L = 10,000$ FT (3,048 M), $\tau = 10$, $\lambda_c = 0.1$ FPS (0.03 M/S)

FIG. 5.—RELATIONSHIP BETWEEN QR_{max} AND η_{ltOp}^* FOR VARIOUS VALUE OF λ^* AND $L = 10,000$ FT (3,048 M), $\tau = 10$, $\lambda_c = 0.01$ FPS (0.003 M/S)

coefficient for the rectangular-shaped spillway. Of course, these would differ from Eqs. 38 and 39 if the openings have shapes other than the assumed V shape and rectangle, respectively.

Optimization of Retarding Layer Location.—In the case of an earthen dam that does not have an erosion retarding layer, the maximum possible reservoir release, Q_{dmp}^* , due to a gradual breach occurs at η_{vm}^* which may be at any elevation within the dam; this elevation depends upon the magnitude of the reservoir surface area, bottom slope, failure rate λ , and C_v . When Q_{dmp}^* occurs, the two factors controlling the rate of discharge through the breach, namely, the head ($\eta_d^* - \eta_v^*$) on the breach and the flow area of the breach must

assume their maximum simultaneous values. Thereafter and until practically all of the reservoir storage is released, the reservoir surface level, y_d^* , decreases because the reservoir outflow, Q_d^* , exceeds the reservoir inflow, Q_u^* .

The optimum elevation, η_{ltOp}^* , of the retarding layer is defined herein as that elevation which minimizes the maximum reservoir outflow, Q_{dm}^* . Thus, by optimally positioning the retarding layer, a maximum reduction in Q_{dm}^* is

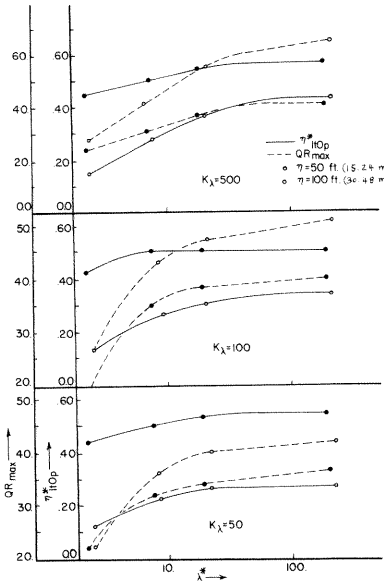


FIG. 6.—RELATIONSHIP BETWEEN QR_{max} AND η_{ltOp}^* FOR VARIOUS VALUES OF λ^* AND $L = 10,000$ FT (3,048 M), $\tau = 10$, $\lambda_c = 0.005$ FPS (0.0015 M/S)

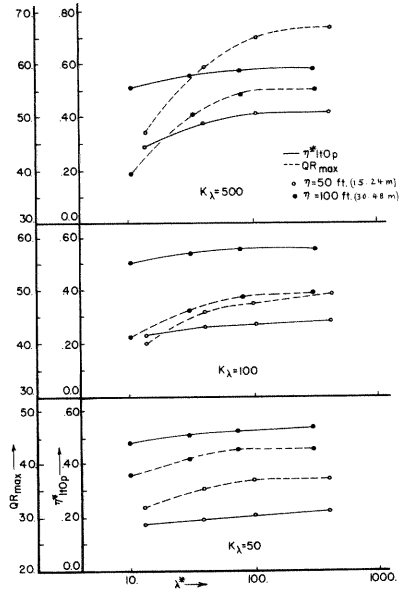


FIG. 7.—RELATIONSHIP BETWEEN QR_{max} AND η_{ltOp}^* FOR VARIOUS VALUES OF λ^* AND $L = 2,000$ FT (610 m), $\tau = 4$, $\lambda_c = 0.1$ FPS (0.03 M/S)

achieved. The reduction is denoted as QR and defined as

$$QR = \frac{(Q_{dm}^* - Q_{dm}^*)_{100}}{Q_{dm}^*} \dots \dots \dots (40)$$

Because QR is a function of η_{lt}^* , an iterative procedure is utilized to determine η_{ltOp}^* within an acceptable accuracy. The function, $QR = QR(\eta_{lt}^*)$, was investigated for a variety of reservoir parameters (L, η, Q_o, λ , etc.) and was found to contain only one maximum value. Thus, the difficulties encountered in the iterative search for η_{ltOp}^* were minimal.

Using an incremental increase $\delta\eta_{lt}^*$, QR_k is computed for each η_{lt}^* position of the retarding layer until QR_{k+1} is greater than QR_k . When this occurs, QR_{max} and the corresponding η_{ltOp}^* exists for a value of η_{lt}^* less than $\eta_{lt}^*_{k+1}$. Then QR_{k+2} and QR_{k+3} are computed, and the final location of QR_{max} is easily

obtained graphically by extending smooth curves through all the computed points (QR, η_{tk}^*) .

NUMERICAL RESULTS

Retarding Layer: Optimal Location and Reduction in Outflow.—Upon applying the numerical simulation model to a range of reservoir sizes, dam heights, initial flowrates, and dam failure rates, prediction curves are obtained for the dimensionless optimal elevation, η_{tOp}^* , of the erosion retarding layer and the

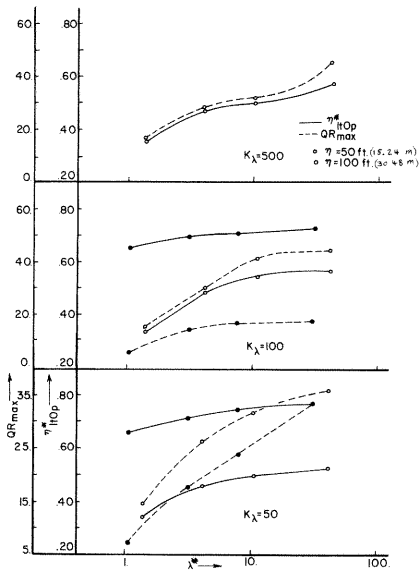


FIG. 8.—RELATIONSHIP BETWEEN QR_{max} AND η_{tOp}^* FOR VARIOUS VALUES OF λ^* AND $L = 2,000$ FT (610 M), $\tau = 4$, $\lambda_c = 0.01$ FPS (0.003 M/S)

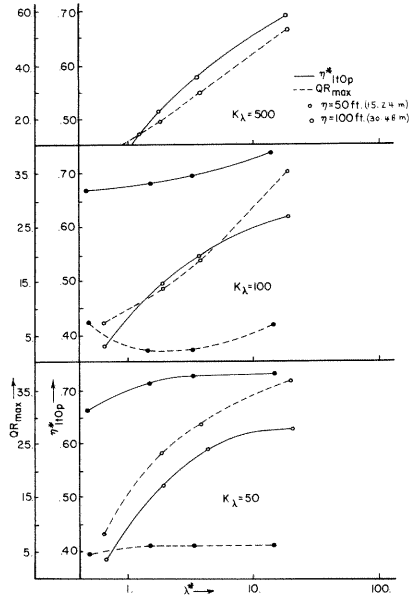


FIG. 9.—RELATIONSHIP BETWEEN QR_{max} AND η_{tOp}^* FOR VARIOUS VALUES OF λ^* AND $L = 2,000$ FT (610 M), $\tau = 4$, $\lambda_c = 0.005$ FPS (0.0015 M/S)

extent of its reduction QR_{max} in the reservoir outflow. The results are functions of the parameters used herein to describe the transient hydraulics associated with the gradual V-breach of an earthfill dam. These parameters consist of the following: geometric parameters ($L, K_1, \tau, \eta, \eta_{sp}$, and η_{ld}); hydraulic parameters (Q_0, n, C_v); and dynamic parameters (λ and K_λ).

The values of η_{tOp}^* and QR_{max} are expressed as functions of the dimensionless failure rate λ^* , as defined by Eq. 19, and for specific values of L, τ, λ_c, η , and K_λ . The prediction curves for η_{tOp}^* and QR_{max} are applicable for the fixed parameters, $K_1 = 1.2, z = 2, \eta_{sp}^* = 0.95, \eta_{ld}^* = 0.02, n = 0.03$, and $C_v = 2.2$. The sensitivity of the prediction curves to variations in these fixed

parameters is examined in a following section.

Prediction curves for η_{ltOp}^* and QR_{max} are shown in Figs. 4-9 for specific values of L , τ , K_λ , and λ_c . The following example illustrates the use of the prediction curves.

When $Q_o = 2,000$ cfs (56.62 m³/s), $L = 10,000$ ft (3048 m), $\eta = 100$ ft (30.48 m), $\lambda_c = 0.01$ fps (0.003 m/s), $\tau = 10$, $K_\lambda = 100$, $K_1 = 1.20$, $z = 2.$, $\eta_{sp}^* = 0.95$, $\eta_{td}^* = 0.02$, $n = 0.03$, and $C_v = 2.2$, the optimum elevation η_{ltOp}^* of an erosion retarding layer and the corresponding reduction QR_{max} in the

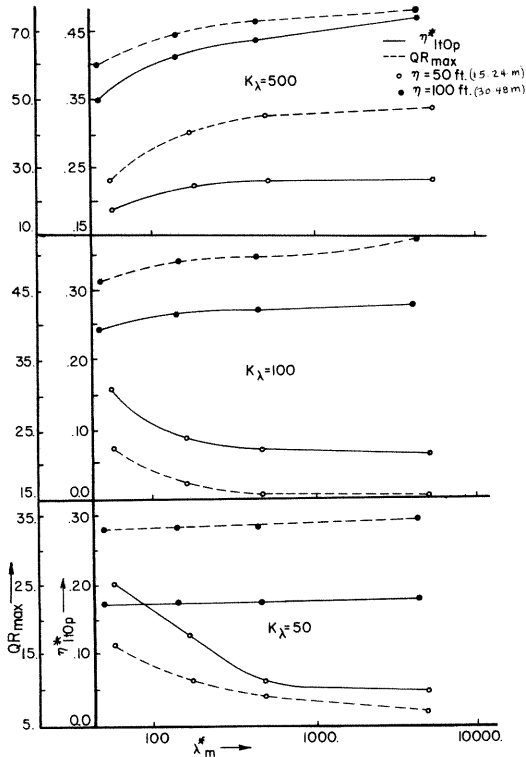


FIG. 10.—RELATIONSHIP BETWEEN QR_{max} AND η_{ltOp}^* FOR VARIOUS VALUES OF λ^* AND $L = 10,000$ FT (3,048 M), $\tau = 10$, $\lambda_m = 0.1$ FPS (0.03 M/S), $y_{dm} = 0.97$, $\eta = 50$ FT (15.24 M), $y_{dm} = 0.91$, $\eta = 100$ FT (30.48 M), AND λ IS AN EXPONENTIAL FUNCTION

maximum possible reservoir release may be obtained from Fig. 5. First, λ^* is computed from Eq. 19, i.e., $\lambda^* = [(10,000)(0.01)/2,000] [(10,000/10) - 2(100)] = 40$. Then a line is extended vertically from the abscissa at $\lambda^* = 40$ to intersect the curves pertaining to $K_\lambda = 100$ and $\eta = 100$ ft (30.48 m) as shown in Fig. 5. Finally, the values of η_{ltOp}^* and QR_{max} are obtained by extending lines horizontally until they intersect the appropriate ordinate axis, and η_{ltOp}^* and QR_{max} are read as 0.46 and 46.8 %, respectively.

Upon examining Figs. 4-9, it is evident that η_{ltOp}^* significantly varies directly with η and K_λ and inversely with L and λ_c . Also, in all except Fig. 4, η_{ltOp}^* varies directly with λ^* .

If the failure rate, λ_c , is very small or L is small, or both, e.g., $L = 2,000$ ft (610 m), the reservoir depth as determined by the numerical model recedes at an increasing rate as the V-breach forms. Under this condition, the maximum possible reservoir release, Q_{dmp}^* , occurs when the rate at which the depth is receding exceeds the failure rate λ_c , i.e. Q_{dmp}^* occurs considerably before the breach achieves its maximum size. Thus, η_{ltOp}^* may assume values in the

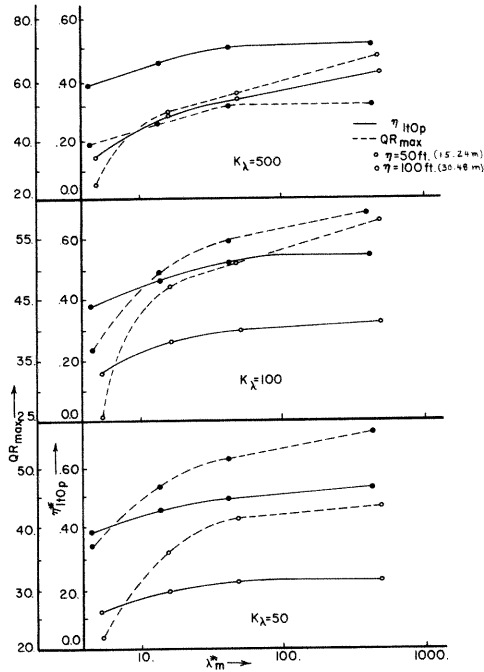


FIG. 11.—RELATIONSHIP BETWEEN QR_{max} AND η_{ltOp}^* FOR VARIOUS VALUES OF λ^* AND $L = 10,000$ FT (3,048 M), $\tau = 10$, $\lambda_m = 0.01$ FPS (0.003 M/S), $y_{dm} = 0.90$, $\eta = 50$ FT (15.24 M), $y_{dm} = 0.58$, $\eta = 100$ FT (30.48 M), AND λ IS AN EXPONENTIAL FUNCTION

range of 0.60 to 0.75. Under this same condition of small values of λ_c or L , or both, the elevation of the erosion retarding layer is critical because it is possible for the layer, if incorrectly positioned above η_{vmp}^* , to cause Q_{dm}^* to exceed Q_{dmp}^* .

In Figs. 4-9, QR_{max} assumes values in the range of 10 % of 65 %. This indicates that significant reductions in the maximum reservoir release from gradually breached dams may be achieved by the presence of an erosion retarding layer which is optimally located. The extent of the reduction, QR_{max} , is primarily related directly to the resistance of the layer to erosion, i.e., K_λ , and to λ^* .

Prediction curves for η_{ltOp}^* and QR_{max} are shown in Figs. 10 and 11 for specific values of L , τ , η , K_λ , λ_m , and y_{dm} . In these, λ is assumed to be an exponential failure rate as described by Eq. 7. The prediction curves in Figs. 10 and 11 are similar to those in Figs. 4 and 5, respectively. The exponential failure rate produced values of η_{ltOp}^* and QR_{max} which are approximately 10% greater than those computed for a constant failure rate. In Figs. 10 and 11, QR_{max} assumes values in the range of 10% to 75%.

TABLE 1.—SENSITIVITY OF η_{ltOp}^* AND QR_{max} TO VARIATIONS IN K_1 , η_{ld}^* , η_{sp}^* , z , τ , C_v , AND n FOR $L = 10,000$ FT (3,048 M), $\tau = 10$, $\lambda_c = 0.01$ FPS (0.003 M/S)

Fixed variable	Value	K_λ	Average Percentage Variation in η_{ltOp}^*		Average Percentage Variation in QR_{max}	
			$\eta = 50$ ft (15.24 m)	$\eta = 100$ ft (30.48 m)	$\eta = 50$ ft (15.24 m)	$\eta = 100$ ft (30.48 m)
(1)	(2)	(3)	(4)	(5)	(6)	(7)
K_1	1.1	100	-12.4	+9.1	+14.0	+8.5
	1.3	100	+1.3	+0.2	-2.1	+8.3
	1.1	500	+1.9	+12.9	+10.0	+2.5
	1.3	500	+5.3	-7.5	-2.6	+2.3
η_{ld}^*	0.01	100	-28.8	-1.9	-10.7	-4.2
	0.05	100	+18.5	+8.0	+17.3	+17.3
	0.01	500	-6.7	-1.5	+1.8	+5.0
	0.05	500	+2.6	+0.9	+6.0	+15.6
η_{sp}^*	0.900	100	-6.5	+0.5	+1.5	+4.2
	0.975	100	-14.0	+3.6	+14.5	+6.3
	0.900	500	+18.0	-10.5	+11.5	+3.4
	0.975	500	+2.7	+18.2	+2.9	+3.5
z	0.0	100	-11.5	-5.4	-5.8	+13.6
	4.0	100	-5.8	+18.0	+1.6	+6.2
	0.0	500	-1.2	-2.8	-7.2	+9.8
	4.0	500	+4.6	+0.5	+13.3	-2.6
n	0.02	100	-7.3	+1.8	+3.4	+6.1
	0.06	100	-5.7	+1.9	+18.0	+2.4
	0.02	500	+1.0	+1.1	+4.1	+5.0
	0.06	500	+1.4	+4.0	+11.9	+5.3
τ	5.0	100	-20.0	-16.6	-17.0	+37.6
	5.0	500	+17.2	-7.0	-14.4	+38.1
C_v	1.0	100	-25.5	-24.0	-37.3	+21.7
	1.0	500	5.5	-36.3	-12.2	+13.3

Sensitivity to Variations in Fixed Parameters.—The sensitivity η_{ltOp}^* and QR_{max} to variations in the values of the fixed parameters is shown in Table 1.

Sensitivity tests indicate that variations in the τ ratio of the width to the length of the prismatic reservoir, and the C_v coefficient of discharge of the V-breach significantly effect the optimal elevation of the retarding layer and the extent of reduction in outflow due to the layer. Variations in the dimensionless thickness, η_{ld}^* , of the retarding layer produce some significant changes in η_{ltOp}^* and QR_{max} as η and K_λ assume smaller values. However, variations in the K_1 ratio of the total length, L' , of the reservoir to length L of the prismatic

portion of the reservoir, dimensionless elevation η_{sp}^* of the spillway crest, side slope z of the trapezoidal reservoir cross section, and Manning roughness coefficient n produce relatively small changes in η_{tOp}^* and QR_{max} .

SUMMARY AND CONCLUSIONS

A conceptual method to reduce flood wave peaks due to overtopping failures of small homogeneous earthfill dams has been introduced. A mathematical model based on a numerical solution of the St. Venant unsteady flow equations is presented for predicting the transient reservoir flow produced by the gradual breach of an earthfill dam.

The extent of reduction in the reservoir outflow from a breached dam due to the presence of a hypothetical erosion retarding layer is presented, along with the optimal elevation of the retarding layer, for a wide range of pertinent geometric, hydraulic, and dynamic parameters. The extent of reduction QR_{max} in the maximum outflow is primarily related directly to the K_λ ratio of the failure rate of the earthfill dam to the failure rate of the erosion retarding layer and to the dimensionless failure rate, λ^* . This reduction can be as significant as 75 %. The dimensionless optimal elevation, η_{tOp}^* , which minimizes the maximum reservoir outflow due to the breach, is related directly to height η of the dam, K_λ , and λ^* and inversely to length L of the prismatic reservoir and to failure rate λ . It is concluded that significant reductions in reservoir releases from breached earthfill dams may be achieved by incorporating an erosion retarding layer within the dam during its construction. Further studies are needed to determine the economic and engineering feasibility of the erosion retarding layer concept and to develop easily applied retarding layer design criteria.

ACKNOWLEDGMENTS

The work upon which this paper is based was supported in part by funds provided under Project No. A-0-35-MO of the United States Department of the Interior, Office of Water Resources Research, as authorized under the Water Resources Act of 1964.

APPENDIX I.—REFERENCES

1. Amein, M., and Fang, C. S., "Implicit Flood Routing in Natural Channels," *Journal of the Hydraulics Division*, ASCE, Vol. 90, No. HY12, Proc. Paper 7773, Dec., 1970, pp. 2481-2500.
2. Amein, M., "Streamflow Routing on Computer by Characteristics," *Water Resources Research*, Vol. 2, No. 1, 1966, pp. 123-130.
3. Baltzer, R. A., and Lai, C., "Computer Simulation of Unsteady Flow in Waterways," *Journal of the Hydraulics Division*, ASCE, Vol. 94, No. HY4, Proc. Paper 6048, July, 1968, pp. 1083-1117.
4. Chow, V. T., *Open-Channel Hydraulics*, McGraw-Hill Book Co., Inc., New York, N.Y., 1959.
5. Fread, D. L., and Harbaugh, T. E., "Gradually Varied Flow Profiles by Newton's Iteration Technique," *Journal of Hydrology*, Vol. 2, 1971, pp. 129-139.
6. Fread, D. L., and Harbaugh, T. E., "Simulation Program for the Transient Hydraulics Produced

- by Gradually Breached Earth Dams," *Hydraulic Series Bulletin*, Civil Engineering Studies, Univ. of Missouri-Rolla, Rolla, Mo., May, 1971.
7. Harbaugh, T. E., "Numerical Techniques for Spatially Varied Unsteady Flow," Report No. 3, 1967, Water Resources Research Center, University of Missouri.
 8. Isaacson, E., Stoker, J. J., and Troesch, A., "Numerical Solution of Flow Problems in Rivers," *Journal of the Hydraulics Division*, ASCE, Vol. 84, No. HY5, Proc. Paper 1810, Oct., 1958, pp. 1810-1818.
 9. Liggett, J. A., "Mathematical Flow Determination in Open Channels," *Journal of the Engineering Mechanics Division*, ASCE, Vol. 94, No. EM4, Proc. Paper 6078, Aug. 1968, pp. 947-963.
 10. Liggett, J. A., and Woolhiser, D. A., "Difference Solutions of the Shallow-Water Equations," *Journal of the Engineering Mechanics Division*, ASCE, Vol. 93, No. EM2, Proc. Paper 5189, Apr., 1967, pp. 39-71.
 11. Lister, M., "The Numerical Solution of Hyperbolic Partial Differential Equations by the Method of Characteristics," *Mathematical Methods For Digital Computers*, A. Ralston and H. S. Wilf, eds., John Wiley & Sons, Inc. New York, N.Y., 1960.
 12. Middlebrooks, T. A., "Earth-Dam Practice in the United States," *Centennial Transactions*, ASCE, Vol. CT, Paper No. 2620, 1953, pp. 697-722.
 13. Strelkoff, T., "The One-Dimensional Equations of Open-Channel Flow," *Journal of the Hydraulics Division*, ASCE, Vol. 95, No. HY3, Proc. Paper 6557, May, 1968, pp. 861-876.
 14. Strelkoff, T., "Numerical Solution of Saint-Venant Equations," *Journal of the Hydraulics Division*, ASCE, Vol. 96, No. HY1, Proc. Paper 7043, Jan. 1970, pp. 223-252.
 15. Stoker, J. J., *Water Waves*, Interscience Publishers, Inc., New York, N.Y., 1966.
 16. Streeter, V. L., and Wylie, E. B., *Hydraulic Transients*, Chap. 15, McGraw-Hill Book Co., Inc., New York, N.Y., 1967.
 17. Vineyard, J. D., "Pinkston Dam Failure," *Mineral Industry News*, Vol. 8, No. 6, June, 1968, pp. 59-61.

APPENDIX II.—NOTATION

The following symbols are used in this paper:

- A = area of channel (reservoir) cross section;
- C_{sp}, C_v = constants defined by Eqs. 38 and 39, respectively;
- C_+, C_- = positive and negative characteristics, respectively;
- c_{sp}, c_v = discharge coefficients for broad crested rectangular and V-shaped weirs, respectively;
- c_1, c_2, c_3 = constants defined by Eq. 12;
- D = hydraulic mean depth;
- d, do, k, l, p, u, uo = subscripts denoting intersection points in $x^* - t^*$ plane;
- g = acceleration due to gravity;
- K_λ = ratio of failure rate of earthfill dam to failure rate of erosion retarding layer;
- $K_1, K_2, K_3, K_4, K_5, K_6$ = constants defined by Eqs. 15-18, 36 and 37, respectively;
- L = length of prismatic section of reservoir;
- L' = length of determining S_o , and defined by Eq. 5;
- L_{sp} = length of emergency spillway crest;
- n = Manning's roughness coefficient;
- Q_d = flow rate at downstream boundary (reservoir outflow);

- Q_{dm} = maximum flow rate at downstream boundary;
 Q_{dmp} = maximum possible flow rate at downstream boundary;
 Q_o = initial steady flow rate in reservoir;
 QR = percentage reduction in Q_{dmp} and defined by Eq. 40;
 QR_{max} = maximum value of QR ;
 R = hydraulic radius;
 S_f = friction slope, slope of energy gradient, defined by Eq. 3;
 S_o = bottom slope of reservoir and defined by Eq. 4;
 T = top width of free surface of channel (reservoir);
 t = time;
 v = average velocity in channel (reservoir);
 v_η = average velocity at downstream boundary when $t = 0$;
 x = distance along channel (reservoir);
 y = depth of flow in channel (reservoir);
 y_d = depth of flow at downstream boundary;
 z = side slope of reservoir cross section;
 $\delta\eta_{lt}^*$ = incremental increase in η_{lt}^* ;
 η = elevation of top of dam, with data line at bottom of dam;
 η_{lb} = elevation of bottom of erosion retarding layer;
 η_{ld} = thickness of erosion retarding layer;
 η_{lt} = elevation of top of erosion retarding layer;
 η_{ltOp} = optimal elevation of top of erosion retarding layer;
 η_{sp} = elevation of emergency spillway crest;
 η_v = elevation of bottom of V-breach when $t = t_d$;
 θ = angle of inclination of channel bottom with horizontal;
 λ = failure rate of dam, rate of formation of V-breach;
 λ_c = constant failure rate during a specified period of time or interval of elevation, η_v ;
 λ_m = estimated maximum failure rate when $\eta_v = \eta_{vmp}$;
 τ = ratio of initial top width to reservoir length L ;
 ϕ = acute central angle of V-breach; and
 $*$ = superscript denoting a dimensionless variable.

9466 SIMULATION OF BREACHED EARTH DAMS

KEY WORDS: Computers; Dams (earth); Hydraulics; Numerical analysis; Open channel flow; Reservoirs; Simulation; Transient flow; Water flow

ABSTRACT: A conceptual method to alleviate flood damages due to overtopping failures of future small earthfill dams is the incorporation of a relatively thin erosion retarding layer within the dam. This paper investigates the potential reduction in the reservoir release due to the proposed erosion retarding layer. The paper provides a method for the determination of an optimal location of the layer so as to minimize the maximum possible reservoir release due to a gradually breached earth dam. The transient reservoir flow is simulated by a numerical model, based upon the solution of the one-dimensional St. Venant unsteady open-channel flow equations. These equations are solved by the method of characteristics, with appropriate boundary conditions incorporated into the solution procedure. The numerical simulation model is used to determine the reduction in reservoir release due to a single retarding layer and its optimal location for a wide range of pertinent geometric, hydraulic and dynamic parameters.

REFERENCE: Fread, Danny L., and Harbaugh, Terence E., "Transient Hydraulic Simulation of Breached Earth Dams," *Journal of the Hydraulics Division*, ASCE, Vol. 99, No. HY1, **Proc. Paper 9466**, January, 1973, pp. 139-154